Molecular Neurobiology

ISSN0893-7648/98/20(1): 45–59/$13.75

Molecular Investigations on the Nicotinic Acetylcholine Receptor

Conformational Mapping and Dynamic Exploration Using Photoaffinity Labeling

Florence Kotzyba-Hibert*, Thomas Grutter, and Maurice Goeldner

Laboratoire de Chimie Bio-Organique, UMR 7514 CNRS, Faculté de Pharmacie-Université Louis Pasteur, 74 Route du Rhin, BP 24, 67401 Illkirch Cedex, France

Abstract

The nicotinic acetylcholine receptor (nAChR) is a well-understood member of the ligand-gated ion channels superfamily. The members of this signaling proteins group, including $5HT_3$, $GABA_A$, glycine, and ionotropic glutamate receptors, are thought to share common secondary, tertiary, and quaternary structures on the basis of a very high degree of sequence similarity. Despite the absence of X-ray crystallographic data, considerable progress on structural analysis of nAChR was achieved from biochemical, mutational, and electron microscopy data allowing the emergence of a three-dimensional image. Photoaffinity labeling and site-directed mutagenesis gave information on the tertiary structure with respect to the agonist/antagonist binding sites, the ion channel, and its selectivity filter.

nAChR is an allosterical protein that undergoes interconversion among several conformational states. Time-resolved photolabeling was used in an attempt to elucidate the structural changes that occur in nAChR on neurotransmitter activation. Tertiary and quaternary rearrangements were found in the cholinergic binding pocket and in the channel lumen, but the structural determinant and the functional link between the binding of agonist and the channel gating remain unknown. Time-resolved photolabeling of the functional activated A state using photosensitive agonists might help in understanding the dynamic process leading to the interconversion of the different states.

Index Entries: Acetylcholine; nicotinic receptors; time-resolved photoaffinity labeling; photosensitive agonists.

Abbreviations: nAChR, nicotinic acetylcholine receptor; ACh, acetylcholine; NCB, noncompetitive channel blocker; [^{3}H]MBTA, *N*-(4-maleimido)benzyltrimethylammonium iodide; [^{3}H]DDF, [^{3}H]*p*-(*N,N*-dimethylamino) benzenediazonium fluoroborate; [^{3}H]CPZ: [^{3}H]chlorpromazine; [^{3}H]TPMP$^+$, [^{3}H]triphenylmethylphosphonium cation; [^{125}I]TID, 3-trifluoromethyl-3-(-*m*-[^{125}I]iodophenyl)diazirine; [^{3}H]QA, [^{3}H]quinacrine azide; [^{3}H]DAF, 2-[^{3}H]diazofluorene; [^{3}H]DCTA, [^{3}H]diazocyclohexadienoylpropyl, trimethyammonium.

* Author to whom all correspondence and reprint requests should be addressed.

Introduction

Nicotinic acetylcholine receptors (nAChRs) are transmembrane glycoproteins, which, in response to the binding of the neurotransmitter acetylcholine (ACh), mediate the translocation of cations across the plasma membrane in which they reside. They form hetero- (or homo) pentamers with various combinations of the 16 different cloned subunits located either in the peripherical system in skeletal muscles (α1, β1, γ, δ, and ε) or in the central nervous system (α2-α9, β2-β4) (reviewed in *(1–3)*. nAChRs are involved in many pathologies, such as congenital myasthenia, family epilepsies, and neurological and psychiatric disorders (Alzheimer's disease, Tourette's syndrome, schizophrenia) (reviewed in *(4,5)*. The knowledge of the structural components of nAChR necessary for agonist binding and agonist-induced changes in structure is very important for therapeutic perspectives.

nAChR is a protein that undergoes allosteric transitions on agonist binding *(6)*. Two distinct sites are involved, on peripherical receptor, in the indirect interaction between the agonist binding site located mainly on both α-subunits and the noncompetitive channel blocker (NCB) site lining in the central axis of ion channel. At least four discrete interconvertible conformational states of the *Torpedo* nAChR have been characterized using fluorescent agonist dansyl-C6-choline, *(7,8)* and electrophysiological recordings of response activation and desensitization *(9)*. These states are called resting (R), active (A), intermediate (I), and desensitized (D) (Fig. 1). Agonist binding leads to channel opening (A) followed by rapid (I) and slow (D) desensitization after prolonged exposure to agonist. The rate of isomerization between R and A lies in the microsecond to millisecond time scale, whereas transition from R to I is in the millisecond to 100-ms time range and from R to D in the minute time range. Native receptor (without any effector) pre-exists mainly in the R state with minor D state <20% *(7,10)*. It may interconvert into D state with competitive antagonists, such as *d*-tubocurarine, or NCBs, such as meproadifen *(11,12)*. According to the conformational

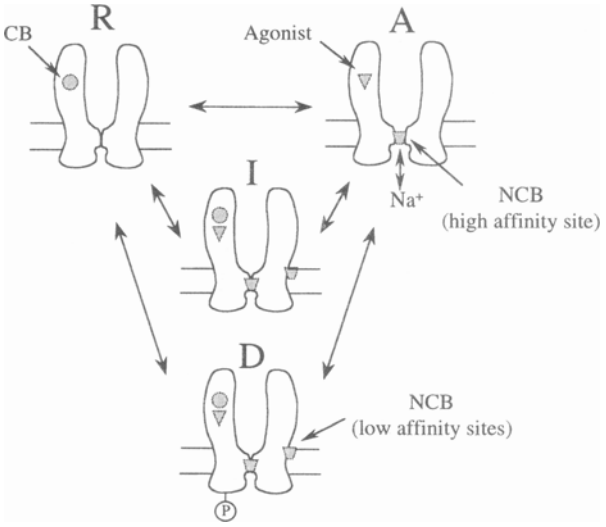

Fig. 1. nAChRs are ligand-gated ion channels that undergo allosteric transitions on effectors activation. A minimum four-state model is proposed by Changeux and coworkers *(7,8)*, including resting (R), active (A), and desensitized (I,D) states. The preferential binding of several classes of ligands to the different states as indicated—CB: competitive blockers; Agonist; NCB: noncompetitive channel blockers (high- and low-affinity binding sites). All these states are discrete, interconvertible, and for some of them, present before ligand binding: native nAChR preexists mainly on the R state with <20% D state *(7,10)*. Allosterical transitions leading to desensitization (I, D states) from R state may occur not only through the actived A state with agonists, but also directly with some antagonist (*d*-tubocurarine), some NCB (Meproadifen) *(11,12)*, and with intracellular phosphorylation (83).

state of the receptor, pronounced differences in affinities are observed, in particular for binding of agonists. For example, the K_D of ACh for the A state is in the 100-μ*M* range and decreases to 10 n*M* for the high-affinity D state *(7,8)*.

Photoaffinity labeling was extensively used to probe the structural changes that occur on desensitization of *Torpedo* nAChR. These experiments used the *Torpedo* ray electric organ, which provides high amounts of nAChR whose structural and functional properties are very close to those of muscular and brain nicotinic receptors, according to recombinant DNA technologies

(13). The ACh binding site was mapped done with the efficient photosensitive probe [^{3}H]DDF *(14–16)*. The labeled amino acid residues were identified in both resting and desensitized states of the receptor *(17)*. Similarly, the NCB [^{125}I]TID has been used to map channel-forming regions of *Torpedo* nAChR in resting and desensitized conformations *(18)*. The interconversion of the resting state to the desensitized state proceeds via the active A state in which the channel remains open for a short period of time (few milliseconds). To trap this transient state by photoaffinity labeling, the development of adapted technologies is required, i.e., rapid mixing techniques coupled with efficient photoirradiation.

Probing the channel-forming regions in the open state has been investigated with time-resolved photolabeling coupled to stopped-flow using different NCBs, such as [^{3}H]chlorpromazine *(19,20)*, [^{3}H]trimethylphenylphosphonium *(21,22)*, or [^{3}H]quinacrine azide *(23–25)*. Structural changes were detected in the quaternary structure of nAChR on activation. However, the functional link between the binding of agonist and the gating of ion channel remains yet to be elucidated.

Conformational Mapping of nAChR in Closed States (R and D)

The ACh Binding Site: Photoaffinity Labeling and Mutagenesis

Muscle and *Torpedo* nAChR formed by pentameric oligomers are composed of five subunits (2α, β, γ/ε, and δ) organized around a central pit. The agonist binding sites are located in the NH_2 terminal domain at the interface of the α-subunits and other subunits (δ or γ). Two clockwise subunit arrangements around the channel are presently suggested: $\alpha_\delta\beta\alpha_\gamma\gamma\delta$ (where β is located between the two α) according photoaffinity labeling of *Torpedo* nAChR with photoactivatable derivatives of an α-neurotoxin from *Naja nigricollis (26)* and electron microscopy *(27)*, and $\alpha_\gamma\gamma\alpha_\delta\delta\beta$ (where γ is located between the two α) from coexpression studies *(28,29)* and crosslinking experiments with photoactivatable derivatives of an α-neurotoxin II from *Naja naja oxiana (30)*. From coexpression experiments, it was shown that α and γ chains expressed together yielded a high-affinity pair, with respect to antagonist binding, and a low-affinity pair for α and δ coexpression, whereas α and β chains coexpression gave no antagonist binding at all *(28,29)*. Similarly, the antagonist *d*-tubocurarine was found to bind with high affinity to the α/γ interface (α_γ) and with low affinity to the α/δ interface (α_δ) *(31)*. On the other hand, recent studies showed that α-Conotoxin M1, isolated from venom of cone snails *(32)*, binds more tighly to the α_γ site than to the α_δ site *(33)*.

Topographical mapping of residues contributing to ACh binding on *Torpedo* nAChR was achieved with the photosensitive antagonist labels [^{3}H]DDF *(15,16)*, [^{3}H]*d*-tubocurarine *(34)*, and with the agonist [^{3}H]nicotine *(35,36)*. From theses studies, three discontinuous domains of the α-subunit centered around αTyr-93 (loop A *(16)*), αTrp-149 (loop B *(15)*), αTyr-190, αCys 192, αCys193, and αTyr-198 (loop C *(15,34,35)*) have been identified (Fig. 2). Convergent data have been obtained on reduced nAChR with the affinity label [^{3}H]MBTA (αCys 192 and αCys193 *(37)*), and on native nAChR with a tritiated analog of lophotoxine (αTyr-190 *(38)*) and [^{3}H]acetylcholine mustard (αTyr-93 *(39)*). More recent work showed that δ- and γ-subunits are also involved in the cholinergic binding pocket as [^{3}H]*d*-tubocurarine photolabeled γTrp55 and δTrp 57 (loop D *(34)*) and [^{3}H]nicotine, γTrp55 (loop D *(36)*). Crosslinking experiments with *S*-(2-[^{3}H] glycylaminoethyl)dithio-2-pyridine *(40)* demonstrated that some γ/δAsp residues lie within 9 Å of the proximal cysteines at position 192 and 193 of the α-subunit. δAsp180 and γAsp174 are thought to be involved in that covalent interaction, since their mutation to Asn dramatically decreased their apparent agonist affinity with greater effect on δAsp180 mutant (loop E) *(41,42)*. Additional amino acid pairs contributing to agonist selectivity were identified on fetal mouse muscle nAChR γ- and δ-subunit chimeras coexpressed with α-subunits *(43)*. Three-dimensional mapping of the agonist bind-

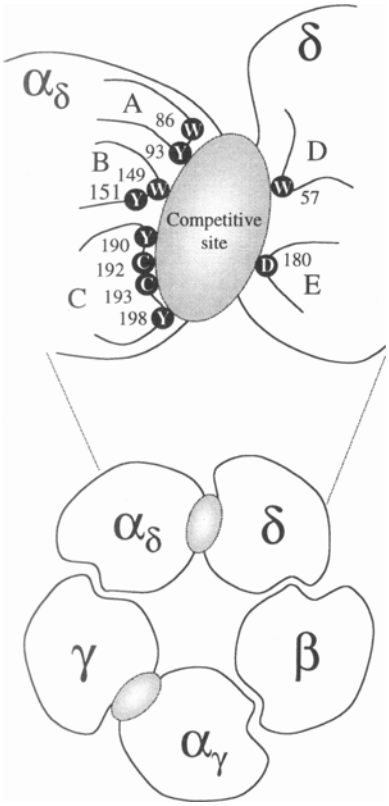

Fig. 2. Mapping of the cholinergic binding pocket on desensitized *Torpedo* nAChR. Pentameric organization of *Torpedo* nAChR subunits around the channel is illustrated here as the clockwise arrangement $\alpha_\gamma\gamma\alpha_\delta\delta\beta$; α_γ and α_δ are the high-affinity and the low-affinity *d*-tubocurarine binding sites, respectively. A five-loop model is proposed (for α_δ here) according to affinity, photoaffinity labeling, crosslinking, and mutagenesis experiments. The amino acids covalently labeled (α_δ and δ) are as follows: [^{3}H]MBTA: αCys 192, αCys 193 in loop C *(37);* [^{3}H]acetylcholine mustard: αTyr 93 in loop A *(39);* [^{3}H]DDF: αTrp 86 and αTyr 93 in loop A, αTryp 149 and αTrp 151 in loop B, αTyr 190, αCys 192, αCys 193, αTyr 198 in loop C *(15,16);* [^{3}H]nicotine: αTyr 190, αCys 192, αTyr 198 in loop C *(35),* and γTryp 55 in loop D *(36);* [^{3}H]lophotoxin analog: αTyr 190 *(38)* in loop C; [^{3}H]*d*-tubocurarine: αTyr 190, αC 192, αTyr 198 in loop C, and γTrp 55, δTrp 57 in loop D *(34).* An additional loop E containing δAsp180 (γAsp174 on α_γ) is proposed to constitute the binding pocket according crosslinking *(40)* and mutagenesis experiments *(41,42).* Amino acids labeled are identified as a single letter in black.

ing cleft on α_δ and α_γ was obtained with these site-directed labels and mutagenesis experiments (Fig. 2). However, photocoupling experiments were performed at equilibrium on the desensitized D state of nAChR (preincubation with [^{3}H]*d*-tubocurarine *(34)* and [^{3}H]nicotine *(35,36)* or with the NCB phencyclidine for [^{3}H]DDF) *(15,16).*

The structural reorganization that occurs in the cholinergic binding domains on desensitization was studied at the amino acid level with [^{3}H]DDF using flash photolysis coupled to a stopped flow apparatus *(17).* nAChR was preincubated with ACh (0.6 μ*M*, 450 ms) to saturate the 17–20% D state existing in the absence of any effector *(7,10)* and then mixed with [^{3}H]DDF for 15 ms and briefly irradiated (<5 ms). Under these conditions, possible effects of [^{3}H]DDF *per se* on receptor interconversions were minimized, and photolabeling of the R state was possible.

The comparison of the labeling pattern obtained in the two states (R and D) confirm the hypothesis of local conformational changes in the cholinergic binding area on desensitization (Fig. 3):

1. The labeling of the α-subunit involved the same set of amino acids as on the R state, but was enhanced in the D state in agreement with the increased affinity for cholinergic ligands.
2. The labeling on peptide loops A (Tyr93) and B (Trp149) increased up to sixfold on D state, but loop C (Tyr 190, Cys 192, Cys 193, and Tyr 198) was labeled in a roughly identical manner.
3. A peptide loop from the δ-subunit was more heavily labeled on D state by [^{3}H]DDF.
4. A peptide loop from the γ-subunit was less intensively labeled on D state by [^{3}H]DDF.

In summary, a reorganization of the tertiary structure of cholinergic binding sites occurred on desensitization with additional interactions, possibly with loops A and B on the α-subunits and with a loop on the δ-subunit.

Site-directed mutageneses were performed on residues photolabeled with DDF on peripherical nAChRs (loop C in *Torpedo (44)* or mouse muscle *(45)* or chick brain α7 homo-oligomeric nAChRs (loops A, B, C *(46,47)* and on residues photolabeled with *d*-tubocurarine on the α 7-

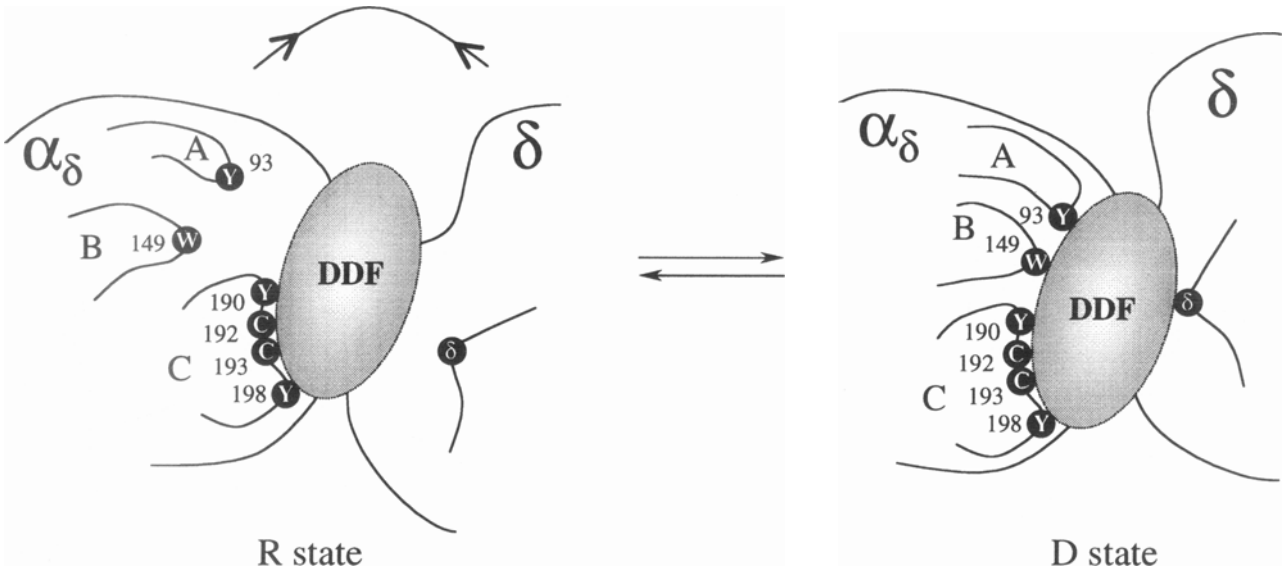

Fig. 3. Conformational mapping of the cholinergic binding pocket with [^{3}H]DDF on R and D states of *Torpedo* nAChR *(17)*. The DDF binding domain on the $\alpha\delta$-subunit, composed of peptide loops from α- and δ-subunits is shown in the R and D states of nAChR. Loops A (αTyr 93) and B (αTrp 149) and the additional loop on the δ-subunit whose labeling increases in the D state are coming closer to DDF, but a loop on γ-subunit moves away (for $\alpha\gamma$ site, not shown). Labeling of loop C (αTyr 190, αCys 192, αCys 193, αTyr 198) remains unchanged on desensitization.

V201-5HT$_3$ chimera nAChR (loop D *(48)*). All these mutations altered agonist affinity and also desensitization process *(46)*, showing their functional importance in cholinergic recognition and in the ionic transmission process.

The NCB Binding Site: Photoaffinity Labeling and Mutagenesis

NCBs block nAChR action by binding to a site or sites distinct from the ACh binding sites. Two classes of binding sites have been described so far: a high-affinity site that appears to bind NCBs with a stoechiometry of 1 per nAChR *(12)* and numerous low-affinity sites (up to 30) located at the interface receptor-membrane lipids (Fig. 1).

According to amphipatic analysis, four hydrophobic segments (M1–M4) common to all nAChR subunits and other ligand-gated ion channels are thought to form membrane-spanning α-helices *(49–51)*. Photoaffinity, affinity labeling with NCBs, and mutagenesis provided insight on the location of the high-affinity NCB site (reviewed in ref. *(52)*. The NCBs [^{3}H]CPZ *(53–55)*, [^{3}H]TPMP$^+$*(56)*, and [^{125}I]TID *(18)* specifically photolabeled, under equilibrium conditions, residues within the M2 sequence. [^{3}H]CPZ and [^{3}H]TPMP$^+$ both label a homologous set of serine residues (αSer248, βSer254, γSer257, and δSer262). [^{3}H]CPZ also labeled leucine and threonine residues (γLeu260, βLeu257, γThr253), suggesting that homologous residues on each of the subunits contribute to the [^{3}H]CPZ binding site. These results support the hypothesis of the helicity of M2 with one-side labeling (Fig. 4). αGlu262 was also identified as the site of incorporation of the affinity label [^{3}H]meproadifen mustard *(57)*. Mutations within the M2 channel domain of the three rings of [^{3}H]CPZ- and [^{125}I]TID-labeled amino acids in the neuronal α7 nAChR

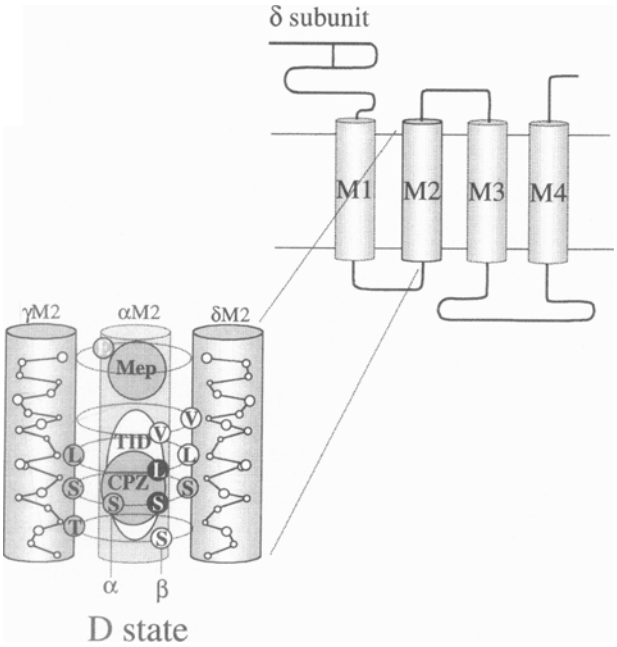

Fig. 4. Mapping of the high-affinity site for NCBs within the ion channel on *Torpedo* nAChR desensitized state D. Each subunit (δ shown here) spans the plasma membrane four times according to literature *(49–51)*. The channel pore is composed of the M2 segments of each subunit, arranged as ideal α-helices. Rings of homologous residues are identified as targets of NCB's (photo)-alkylation. [^{3}H]CPZ binding site extends over the rings of serines (αSer248, βSer254, γSer257, δSer262), leucine (γLeu260, βLeu257), and threonine (γThr 253) *(53–55)*. [^{3}H]TPMP$^+$ photolabeled the CPZ-serine ring *(56)*, but the [^{125}I]TID binding site overlaps the CPZ/TPMP$^+$ binding site (βSer 254) and extends to the upper ring of valine (βVal261 and δVal269) and the lower serine (βSer 250) *(18)*. The affinity label [^{3}H]meproadifen mustard alkylates αGlu262 at the upper part of M2 *(57)*. Amino acids labeled with [^{3}H]CPZ are in gray, with [^{125}I]TID in white, common to [^{3}H]CPZ and [^{125}I]TID in black.

(Thr244Gln, Leu247Thr, and Val251Thr, respectively, α7 numbering) affected the apparent affinity not only of channel blockers, but also that of agonists and competitive antagonists. It also abolished desensitization of α7 mutants *(58)*. In particular, a new conducting desensitized state was detected in the mutant Leu247Thr, activated by a low ACh concentration and several competitive antagonist of the wild type *(58,59)*. Mutations of only two residues (Leu to Cys on the α-subunit) from the leucine ring in mouse muscle nAChR increased apparent ACh affinity and slightly reduced desensitization *(60)*. This leucine ring of amino acids would thus play a critical role in the closing of the ion channel on desensitization.

In summary, mutations of residues belonging to the cholinergic binding site or to the αM2 domain can affect the coupling between the binding site and the channel, possibly by changing the rate (or equilibrium constant) for interconversion between open and closed channel states with no associated changes in the intrinsic properties of the allosteric states. A reconsidered allosteric model was proposed to explain the large diversity of functional properties and the widely pleiotropic phenotypes, which arise from point mutations in nAChR subunits *(61)*.

[^{125}I]TID photolabeling provided the first evidence, at the molecular level, for an agonist-dependent rearrangement of the M2 α-helices *(18)*. Whereas homologous aliphatic residues (βLeu257, δLeu265, βVal261, and γVal269) in the M2 region of three subunits were labeled without agonist, their labeling was reduced (90%) and broadened to a set of CPZ-labeled residues near the cytoplasmic domain of M2 (βSer250, βSer254) in the presence of the agonist carbamylcholine. A model of the nAChR was proposed where [^{125}I]TID incorporates similarly to [^{3}H]CPZ into the amino-terminal half of βM2 and δM2 facing the channel. In the absence of agonist, [^{125}I]TID was tighly bound at the level of these unreactive Leu and Val residues. On agonist activation, a broad pattern of labeling was obtained involving residues above and below the Leu and Val rings. These results demonstrated a wideness of the pore in the desensitized state. The inefficiency of labeling in the presence of agonist was possibly owing to the quenching of photogenerated carbene by water molecules that have access to the pore in the desensitized state *(18)*. This new set of photolabeled residues might be the result of a mixture of photolabel-

ing patterns of nAChR in the resting and desensitized states, since TID stabilizes the resting state probably through strong and tight hydrophobic interactions with residues of the hydrophobic rings *(18)*. Rapid-mixing experiments show that TID might act either on the resting or desensitized state in preference to the open state of nAChR *(62)*. 2-[^{3}H]diazofluorene ([^{3}H]DAF) photolabeling recently provided further characterization of an agonist-induced rearrangement of the ion channel. In the absence of agonist, [^{3}H]DAF specifically labels βVal261 and δVal269, but in the presence of agonist, a 90% reduction of labeling was observed and residues closer to the cytoplasmic end of M2 were labeled (βLeu257, βAla258, δSer262, and δLeu265) *(63)*.

The ACh and the NCB Binding Sites: NMR and X-ray Crystallography of Ligand Binding Fragments

Biotechnological approaches were recently developed to probe the molecular structure of ligand-gated ion channel binding sites. The crystal structure of the ligand binding core S1S2 expressed in *Escherichia coli* of the ionotropic glutamate receptor iGluR$_2$ complexed with kainate was resolved with high resolution *(64)*. Information provided by this structure is essential for the understanding of receptor–agonist interactions and binding specificity. In addition, new insights on ligand-induced channel gating and allosteric effector action emerged from these data.

The NMR structure of recombinant M2 segments of nAChR (δ-subunit) and N-methyl-D-aspartate receptor (NMDAR) (NRI subunit) reconstituted in bilayers were produced *(65)*. Cation-selective channels were formed as monitored with single-channel recording *(65,66)*. A model was proposed for M2 location in the lipid bilayer and a funnel-like architecture for channel with the wide opening on the N-terminal intracellular side was suggested, assuming a symmetric pentameric arrangement of M2 helices. These alternative approaches, complementary to photoaffinity labeling, in the attempt to probe the molecular structure of protein fragments might be used in the future for dynamic studies.

Conformational Mapping of nAChR in the Open Activated State A

Electron Microscopy

A study by Unwin *(67)* showed that agonist binding to nAChR produced structural transitions. Electron images of *Torpedo* nAChR, crystallized in tubular vesicles at 9-Å resolution, were analyzed before and after brief exposure (<5 ms) to ACh. Comparison of the open and closed channel forms gives direct insight into the structural disturbances occurring in the nAChR during agonist activation and channel opening.

In the extracellular part of nAChR, sets of three rods are seen in each subunit, about 30 Å above the membrane bilayer. They form a cavity that is more pronounced in the α-subunits and is proposed to represent the ligand binding site. After ACh exposure, this cavity in the α_δ-subunit disappears in the activated structure, but the β-subunit moves away from the α_δ-subunit toward the α_γ-subunit. This coordination of structural responses of the two α-subunits is proposed to be central to the cooperative mechanism responsible for channel opening.

In the membrane-spanning part of nAChR, five rods of density formed a wall around a pore. They can be assigned to the 25- to 35-Å long α-helical M2 segment of each subunit according to their size and exposition to the lumen of the pore. The rest of the molecule was shown as a rim of continuous density facing the lipids, likely assumed to be composed of β-sheets or turns. This observation was in contradiction to [^{125}I]TID photoalkylation of receptor parts in interaction with phospholipids where M3 and M4 were identified as α-helices *(68)*. In the closed state, the M2 helices kink about their midpoint and come close to the central axis of the pore to form the gate composed of large side-chain residues corresponding probably to the leucine ring photoalkylated by NCBs (Fig.

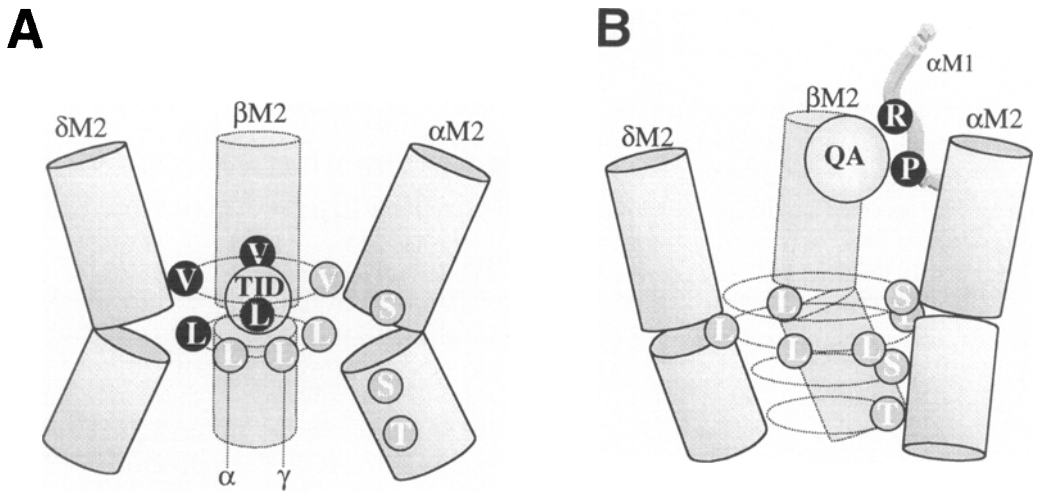

Fig. 5. Mapping of the high-affinity site for NCBs within the ion channel on *Torpedo* nAChR R and A states. 2. On the closed R state, M2 segments are visualized as α-helices kinked about their midpoint according to Unwin *(67)*. [^{125}I]TID binding site on R state is located within the rings of valine (βVal261, δVal269) and leucine (βLeu257, δLeu265) *(18)*. 3. [^{3}H]QA binding site on A state: according to Unwin *(67)*, on agonist activation, the pore opens drawing away gate-forming side chains (Leu in gray) from the central axis. This movement allows polar hydroxylic residues to face the channel (αSer and αThr in gray), thus falicitating ion translocation. A part of M1, schematically represented here as a loop, fills the gap owing to α-helices M2 rearrangement and contributes to [^{3}H]QA photolabeling (αArg209, αPro 211) in the open channel state A *(24,25)*. Amino acids labeled are represented as a single letter in black.

5A). On activation, helices could bend tangentially to the central axis and associate side to side, thus opening the pore, drawing gate-forming side chains away from the central axis and allowing polar hydroxylic residues to become exposed in the lumen (Fig. 5B).

Time-Resolved Photolabeling of the NCB Binding Site in the A Open State

To trap the transient A open state of nAChR, rapid-mixing photolabeling apparatuses were developed by several groups (Fig. 6) *(19,20,22,23)*. Heidmann and Changeux studied the kinetics of photolabeling of [^{3}H]CPZ with *Torpedo* nAChR in the 100-ms to seconds time range *(19,20)*. The four subunits were labeled after rapid mixing with ACh and brief (20 ms) UV irradiation. The agonist-dependent, rapid association of [^{3}H]CPZ took place with nAChR in its open-channel conformation, whereas association with closed state (agonist-induced desensitized state) was very slow owing to a structural barrier that restricts the accessibility of the NCB. High-energy pulsed laser coupled to a rapid-mixing photolabeling apparatus *(22)* was used to probe the channel with [^{3}H]TPMP^{+} on a ms time resolution (dead-time 2.4 ms). In the resting and activated states, most of the label was incorporated into the α-subunit, whereas δ (and to a lesser extent β) reacted with the probe on agonist-induced desensitized nAChR *(21,69)*.

Torpedo nAChR was also photoalkylated with [^{3}H]QA on a 20- to 200-ms time scale. α- and β-chains were labeled predominantly with an enhancement after brief exposure to ACh. This labeling decreased after long exposure to ACh *(23)*. nAChR was photolabeled with [^{3}H]QA 20 ms after ACh addition: under these conditions, the kinetics of the specific labeling were consistent with the preferential labeling

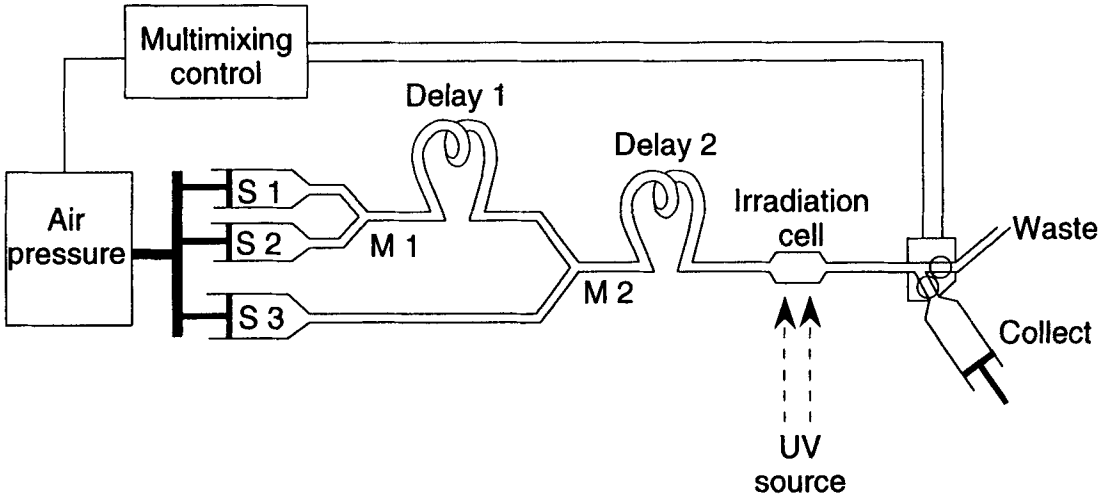

Fig. 6. Schematic representation of rapid-mixing photolysis apparatus for time-resolved photolabeling. Combined stopped-flow and multimixing spectrophotometers with efficient UV source (laser or high-pressure mercury lamp) were constructed and used for rapid-mixing photolabeling *(19,22,23)*. The sequential rapid mixing of up to three solutions (prepared in drive syringes S1–S3) was performed in mixing chambers M1 and M2, with possible variation of the length of the delay tube, 1 and 2, and was time-controlled by multimixing control module. The mixed solutions were irradiated while passing in the irradiation cell and were collected in the collect syringe. Flow rate was adjusted by varying the pressure of the air ram. In [^{3}H]DDF's rapid mixing experiments *(17)*, S1 = *Torpedo* nAChR, S2 = acetylcholine, and S3 = [^{3}H]DDF.

of the open state A, since the specific labeling reached a maximum at 50 μM (value close to its apparent affinity for activation of ion flux). Residues αArg209 and αPro211 of M1 segment were labeled on the α-subunits *(24,25)*, demonstrating that the extracellular part of M1 is involved in the NCB binding site in its open state. To reconcile the labeling by [^{3}H]QA of the M1 region of α and the labeling with [^{3}H]CPZ and other NCBs of the M2 regions of α, β, and γ, several hypotheses were proposed:

1. They all bind to the same site, but photoreact with different residues, since photogenerated species display quite different reactivities (nitrene for QA, carbene for TID, and probably undefined radical species for CPZ and $TPMP^+$.
2. They bind to two different NCB sites, since αSer248 was too distant (2 nm at least) from the αArg209-Pro211 pair assuming that M1 and M2 are α-helices oriented normally to the membrane.
3. QA binds to a site on the open receptor that is in contact with lipid bilayer and not in the channel lumen *(70)*.
4. M1 becomes accessible from the inside of the channel when the receptor is in the active state.

According to recent literature *(71)*, the most reliable hypothesis would be that residues identified as the reactive sites for QA are located in the channel lumen rather than at a lipid interface site. On agonist activation and channel opening, membrane-spanning peptides other than M2, such as a part of M1, may be involved in filling the gap, assuming that all or a part of M1 is not an α-helix (Fig. 5B). Using the substituted-cysteine accessibility method (SCAM), Karlin and collaborators showed on mouse-muscle nAChR that some αM1 *(72)* and βM1 *(73)* residues (N-terminal third) contribute to the lining of the channel and undergo structural changes during gating. M1 appeared not to be helical based on photolabeling with [^{125}I]TID of phospholipid interacting parts of nAChR *(68)*. Furthermore, αCys222, which was supposed to be located at the center of the α helix M1, was found to be closed to the membrane–water interface, suggesting an irregular

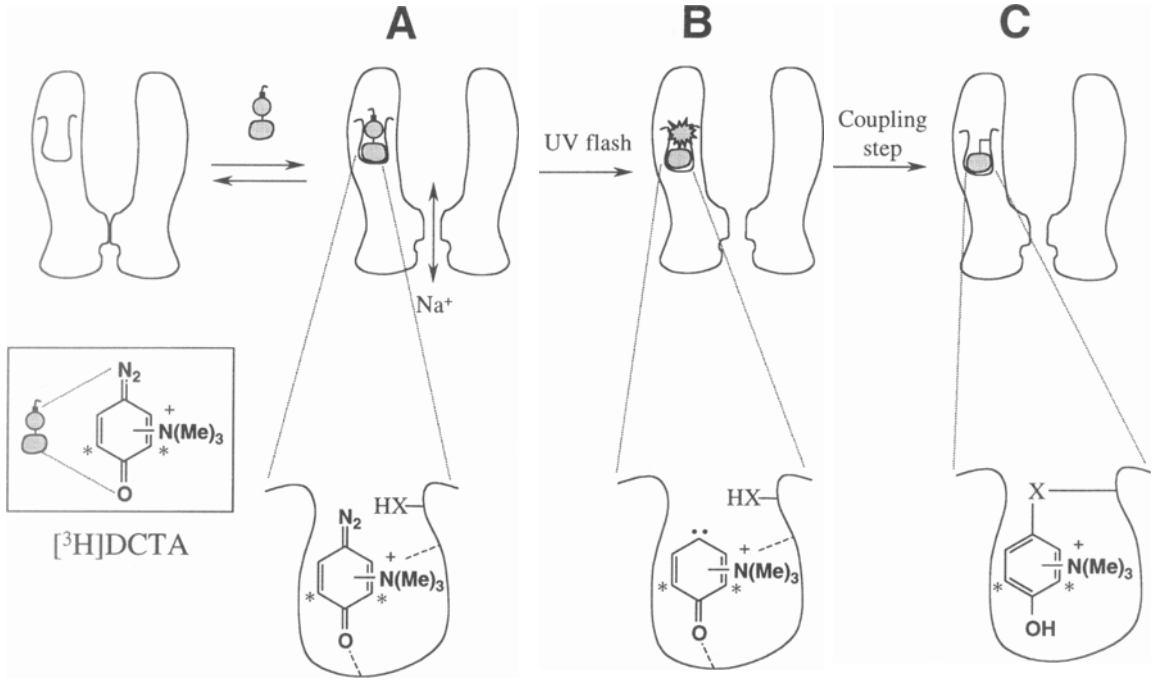

Fig. 7. Dynamical mapping of the activated state A of nAChR with a photosensitive agonist. Rapid mixing of nAChR with the photoprobe triggers channel opening **(A)** on an ms time scale and in the dark. The activated receptor is then UV-irradiated while passing in the irradiation cell **(B),** and the highly reactive species photogenerated *in situ* in the cholinergic binding pocket reacts covalently and instantaneously with surrounding residues **(C).** A hypothetical mechanism is proposed for rapid coupling of photogenerated carbene from the diazocyclohexadienone [^{3}H]DCTA with the cholinergic binding pocket. The carbonyl group and the charged quaternary ammonium of [^{3}H]DCTA mimic the pharmacophore, ensuring cholinergic recognition. X-H represents any amino acid belonging to the cholinergic binding pocket.

structure for M1 *(74).* M1 would then probably contain a β strand or α-helix segments spanning the membrane in a different way than linear α-helix. Finally, molecular modeling of nAChR was performed taking into account recent literature *(75,76),* and in this model, M1 was built as a three-strand β-sheet.

New Perspectives: Toward the Dynamic Mapping of nAChR

The topographical mapping of the cholinergic binding site and of the ion channel has been elucidated using photoaffinity labeling and mutagenesis, as shown here. Nevertheless, we do not know the important structural details of the ligand binding pocket that triggers the channel gating on agonist binding. Time-resolved photolabeling of the ACh binding site in its active A state using photosensitive agonists might help to elucidate the structural determinants of channel gating. Labeling the A state represents a challenge, since the probe must necessarily be an agonist possessing photochemical properties compatible with ms time-resolved photolabeling (for review, see *(77)*). Figure 7 illustrates the different steps necessary for alkylation of the active state. For this purpose, [^{3}H]nicotine is not ideal, because it suffers from extremely low labeling efficiency under equilibrium conditions (~1%) *(35).* New

photosensitive agonists containing an aryldiazonium salt were developed in our laboratory, which allowed very efficient labeling of *Torpedo* nAChR (>50% ACh binding sites labeled *(78)*). Preliminary rapid mixing experiments pointed out different patterns of labeling according to the state of nAChR (R or D). However, a broad labeling pattern involving all four subunits was observed, probably owing to the size and flexibility of the used probe (14.5 Å in the extended conformation). Therefore, in an attempt to analyze more precisely the conformational transitions within the agonist binding site on nAChR activation, we proposed recently a novel class of photosensitive agonists of adapted size and reactivity *(79)*. They combine a highly photosensitive moiety with a quaternary ammonium group necessary for cholinergic recognition. The photoprobe 4-diazo-cyclohexa-2,5-dienone generates on UV irradiation extremely reactive carbenic species able to react efficiently with a nonactivated C–H bond *(80)* (Fig. 7). One of these photoprobes, DCTA, was shown to be a functional agonist *(81)*. [^{3}H]DCTA was synthetized and used successfully to photoalkylate the ACh binding site of *Torpedo* nAChR with satisfying incorporation, mainly on the α-subunits. Preliminary experiments using a 20-ns laser flash pulse led to 8% specific labeling of the agonist binding sites on D state *(82)*.

Future experiments with [^{3}H]DCTA using time-resolved photolabeling might represent a decisive step toward resolution of the dynamic photolabeling of the nAChR. A more precise molecular understanding of conformational changes underlying the dynamic structural processes in cholinergic neurotransmission should be possible by comparing the topography of the cholinergic binding area before, during, and after agonist activation.

Acknowledgments

We thank M. Hibert and J. L. Galzi for critically reading the manuscript. Financial support was from the Centre National de la Recherche Scientifique, the Région Alsace and the Association Francaise contre les Myopathies.

References

1. Galzi J. L. and Changeux J. P. (1995) Neuronal nicotinic receptors: molecular organization and regulations. *Neuropharmacology* **34,** 563–582.
2. Role L. W. and Berg D. K. (1996) Nicotinic receptors in the development and modulation of CNS synapses. *Neuron* **16,** 1077–1085.
3. Hucho F., Tsetlin V. I., and Machold J. (1996) The emerging three-dimensional structure of a receptor. The nicotinic acetylcholine receptor. *Eur. J. Biochem.* **239,** 539–557.
4. Lena C. and Changeux J. P. (1998) Allosteric nicotinic receptors, human pathologies. *J. Physiol. Paris* **92,** 63–74.
5. Engel A. G., Ohno K., and Sine S. M. (1998) Congenital myasthenic syndromes: experiments of nature. *J. Physiol. Paris* **92,** 113–117.
6. Changeux J. P. and Edelstein S. J. (1998) Allosteric receptors after 30 years. *Neuron* **21,** 959–980.
7. Heidmann T. and Changeux J. P. (1979) Fast kinetic studies on the interaction of a fluorescent agonist with the membrane-bound acetylcholine receptor from *Torpedo* marmorata. *Eur. J. Biochem.* **94,** 255–279.
8. Heidmann T., Bernhardt J., Neumann E., and Changeux J. P. (1983) Rapid kinetics of agonist binding and permeability response analyzed in parallel on acetylcholine receptor rich membranes from *Torpedo* marmorata. *Biochemistry* **22,** 5452–5459.
9. Feltz A. and Trautmann A. (1982) Desensitization at the frog neuromuscular junction: a biphasic process. *J. Physiol.* **322,** 257–272.
10. Boyd N. D. and Cohen J. B. (1980) Kinetics of binding of [3H]acetylcholine and [3H]carbamoylcholine to *Torpedo* postsynaptic membranes: slow conformational transitions of the cholinergic receptor. *Biochemistry* **19,** 5344–5353.
11. Krodel E. K., Beckman R. A., and Cohen J. B. (1979) Identification of a local anesthetic binding site in nicotinic post-synaptic membranes isolated from *Torpedo* marmorata electric tissue. *Mol. Pharmacol.* **15,** 294–312.
12. Heidmann T., Oswald R. E., and Changeux J. P. (1983) Multiple sites of action for noncompetitive blockers on acetylcholine receptor rich membrane fragments from torpedo marmorata. *Biochemistry* **22,** 3112–3127.

13. Numa S. (1989) A molecular view of neurotransmitter receptors and ionic channels. *Harvey Lecture Series* **83,** 121–165.
14. Langenbuch-Cachat J., Bon C., Mulle C., Goeldner M., Hirth C., and Changeux J. P. (1988) Photoaffinity labeling of the acetylcholine binding sites on the nicotinic receptor by an aryldiazonium derivative. *Biochemistry* **27,** 2337–2345.
15. Dennis M., Giraudat J., Kotzyba-Hibert F., Goeldner M., Hirth C., Chang J. Y., et al. (1988) Amino acids of the *Torpedo* marmorata acetylcholine receptor alpha subunit labeled by a photoaffinity ligand for the acetylcholine binding site. *Biochemistry* **27,** 2346–2357.
16. Galzi J. L., Revah F., Black D., Goeldner M., Hirth C., and Changeux J. P. (1990) Identification of a novel amino acid alpha-tyrosine 93 within the cholinergic ligands-binding sites of the acetylcholine receptor by photoaffinity labeling. Additional evidence for a three-loop model of the cholinergic ligands-binding sites. *J. Biol. Chem.* **265,** 10,430–10,437.
17. Galzi J. L., Revah F., Bouet F., Menez A., Goeldner M., Hirth C., et al. (1991) Allosteric transitions of the acetylcholine receptor probed at the amino acid level with a photolabile cholinergic ligand. *Proc. Natl. Acad. Sci. USA* **88,** 5051–5055.
18. White B. H. and Cohen J. B. (1992) Agonist-induced changes in the structure of the acetylcholine receptor M2 regions revealed by photoincorporation of an uncharged nicotinic noncompetitive antagonist. *J. Biol Chem.* **267,** 15,770–15,783.
19. Heidmann T. and Changeux J. P. (1984) Time-resolved photolabeling by the noncompetitive blocker chlorpromazine of the acetylcholine receptor in its transiently open and closed ion channel conformations. *Proc. Natl. Acad. Sci. USA* **81,** 1897–1901.
20. Heidmann T. and Changeux J. P. (1986) Characterization of the transient agonist-triggered state of the acetylcholine receptor rapidly labeled by the noncompetitive blocker [3H]chlorpromazine: additional evidence for the open channel conformation. *Biochemistry* **25,** 6109–6113.
21. Fahr A., Lauffer L., Schmidt D., Heyn M. P., and Hucho F. (1985) Covalent labeling of functional states of the acetylcholine receptor. Effects of antagonists on the receptor conformation. *Eur. J. Biochem.* **147,** 483–487.
22. Muhn P., Fahr A., and Hucho F. (1984) Rapid laser flash photoaffinity labeling of binding sites for a noncompetitive inhibitor of the acetylcholine receptor. *Biochemistry* **23,** 2725–2730.
23. Cox R. N., Kaldany R. R., DiPaola M., and Karlin A. (1985) Time-resolved photolabeling by quinacrine azide of a noncompetitive inhibitor site of the nicotinic acetylcholine receptor in a transient, agonist-induced state. *J. Biol. Chem.* **260,** 7186–7193.
24. DiPaola M., Kao P. N., and Karlin A. (1990) Mapping the alpha-subunit site photolabeled by the noncompetitive inhibitor [3H]quinacrine azide in the active state of the nicotinic acetylcholine receptor. *J. Biol. Chem.* **265,** 11,017–11,029.
25. Karlin A. (1991) Explorations of the nicotinic acetylcholine receptor. *Harvey Lectures* 71–107.
26. Chatrenet B., Tremeau O., Bontems F., Goeldner M. P., Hirth C. G. and Menez A. (1990) Topography of toxin-acetylcholine receptor complexes by using photoactivatable toxin derivatives. *Proc Natl Acad Sci USA* **87,** 3378–3382.
27. Kubalek E., Ralston S., Lindstrom J., and Unwin N. (1987) Location of subunits within the acetylcholine receptor by electron image analysis of tubular crystals from *Torpedo* marmorata. *J. Cell. Biol.* **105,** 9–18.
28. Blount P. and Merlie J. P. (1989) Molecular basis of the two nonequivalent ligand binding sites of the muscle nicotinic acetylcholine receptor. *Neuron* **3,** 349–357.
29. Sine S. M. and Claudio T. (1991) Gamma- and delta-subunits regulate the affinity and the cooperativity of ligand binding to the acetylcholine receptor. *J. Biol. Chem.* **266,** 19,369–19,377.
30. Machold J., Weise C., Utkin Y., Franke P., Tsetlin V., and Hucho F. (1995) A new class of photoactivatable and cleavable derivatives of neurotoxin II from Naja maja oxiana. *Eur. J. Biochem.* **228,** 947–954.
31. Pedersen S. E. and Cohen J. B. (1990) d-Tubocurarine binding sites are located at alpha-gamma and alpha-delta subunit interfaces of the nicotinic acetylcholine receptor. *Proc Natl Acad Sci USA* **87,** 2785–2789.
32. Myers R. A., Zafaralla G. C., Gray W. R., Abbott J., Cruz L. J., and Olivera B. M. (1991) alpha-Conotoxins, small peptide probes of nicotinic acetylcholine receptors. *Biochemistry* **30,** 9370–9377.
33. Sine S. M., Kreienkamp H. J., Bren N., Maeda R., and Taylor P. (1995) Molecular dissection of

subunit interfaces in the acetylcholine receptor: identification of determinants of alpha-conotoxin M1 selectivity. *Neuron* **15,** 205–211.
34. Chiara D. C. and Cohen J. B. (1997) Identification of amino acids contributing to high and low affinity *d*-tubocurarine sites in the *Torpedo* nicotinic acetylcholine receptor. *J. Biol. Chem.* **272,** 32,940–32,950.
35. Middelton R. E. and Cohen B. C. (1991) Mapping of the acetylcholine binding site of the nicotinic acetylcholine receptor: [3H]Nicotine as an agonist photoaffinity label. *Biochemistry* **30,** 6987–6997.
36. Chiara D. C., Middleton R. E., and Cohen J. B. (1998) Identification of tryptophan 55 as the primary site of [3H]nicotine photoincorporation in the gamma-subunit of the Torpedo nicotinic acetylcholine receptor. *FEBS Lett.* **423,** 223–226.
37. Kao P. N., Dwork A. J., Kaldany R. R., Silver M. L., Wideman J., Stein S., et al. (1984) Identification of the alpha subunit half-cystine specifically labeled by an affinity reagent for the acetylcholine receptor binding site. *J. Biol. Chem.* **259,** 11,662–11,665.
38. Abramson S. N., Li Y., Culver P., and Taylor P. (1989) An analog of lophotoxin reacts covalently with Tyr190 in the alpha-subunit of the nicotinic acetylcholine receptor. *J. Biol. Chem.* **264,** 12,666–12,672.
39. Cohen J. B., Sharp S. D., and Liu W. S. (1991) Structure of the agonist-binding site of the nicotinic acetylcholine receptor. [3H]acetylcholine mustard identifies residues in the cation-binding subsite. *J. Biol. Chem.* **266,** 23,354–23,364.
40. Czajkowski C. and Karlin A. (1991) Agonist binding site of Torpedo electric tissue nicotinic acetylcholine receptor. A negatively charged region of the delta subunit within 0.9 nm of the alpha subunit binding site disulfide. *J. Biol. Chem.* **266,** 22,603–22,612.
41. Martin M., Czajkowski C., and Karlin A. (1996) The contributions of aspartyl residues in the acetylcholine receptor gamma and delta subunits to the binding of agonists and competitive antagonists. *J. Biol. Chem.* **271,** 13,497–13,503.
42. Martin M. D. and Karlin A. (1997) Functional effects on the acetylcholine receptor of multiple mutations of gamma Asp174 and delta Asp180. *Biochemistry* **36,** 10,742–10,750.
43. Prince R. J. and Sine S. M. (1996) Molecular dissection of subunit interfaces in the acetylcholine receptor. Identification of residues that determine agonist selectivity. *J. Biol. Chem.* **271,** 25,770–25,777.
44. O'Leary M. E. and White M. M. (1992) Mutational analysis of ligand-induced activation of the *Torpedo* acetylcholine receptor. *J. Biol. Chem.* **267,** 8360–8365.
45. Tomaselli G. F., McLaughlin J. T., Jurman M. E., Hawrot E., and Yellen G. (1991) Mutations affecting agonist sensitivity of the nicotinic acetylcholine receptor. *Biophys. J.* **60,** 721–727.
46. Galzi J. L., Bertrand D., Devillers-Thiery A., Revah F., Bertrand S., and Changeux J. P. (1991) Functional significance of aromatic amino acids from three peptide loops of the alpha 7 neuronal nicotinic receptor site investigated by site-directed mutagenesis. *FEBS Lett.* **294,** 198–202.
47. Sine S. M., Quiram P., Papanikolaou F., Kreienkamp H. J., and Taylor P. (1994) Conserved tyrosines in the alpha subunit of the nicotinic acetylcholine receptor stabilize quaternary ammonium groups of agonists and curariform antagonists. *J. Biol. Chem.* **269,** 8808–8816.
48. Corringer P. J., Galzi J. L., Eisele J. L., Bertrand S., Changeux J. P., and Bertrand D. (1995) Identification of a new component of the agonist binding site of the nicotinic alpha 7 homooligomeric receptor. *J. Biol. Chem.* **270,** 11,749–11,752.
49. Devillers-Thiery A., Giraudat J., Bentaboulet M., and Changeux J. P. (1983) Complete mRNA coding sequence of the acetylcholine binding alpha-subunit of *Torpedo* marmorata acetylcholine receptor: a model for the transmembrane organization of the polypeptide chain. *Proc. Natl. Acad. Sci. USA* **80,** 2067–2071.
50. Claudio T., Ballivet M., Patrick J., and Heinemann S. (1983) Nucleotide and deduced amino acid sequences of *Torpedo* californica acetylcholine receptor gamma subunit. *Proc. Natl. Acad. Sci. USA* **80,** 1111–1115.
51. Noda M., Takahashi H., Tanabe T., Toyosato M., Kikyotani S., Furutani Y., et al. (1983) Structural homology of Torpedo californica acetylcholine receptor subunits. *Nature* **302,** 528–532.
52. Bertrand D., Galzi J. L., Devillers-Thiery A., Bertrand S., and Changeux J. P. (1993) Stratification of the channel domain in neurotransmitter receptors. *Curr Opin Cell Biol* **5,** 688–693.
53. Giraudat J., Dennis M., Heidmann T., Chang J. Y., and Changeux J. P. (1986) Structure of the high-affinity binding site for noncompetitive blockers of the acetylcholine receptor: serine-262 of the delta subunit is labeled by [3H]chlor-

promazine. *Proc. Natl. Acad. Sci. USA* **83,** 2719–2723.
54. Giraudat J., Dennis M., Heidmann T., Haumont P. Y., Lederer F., and Changeux J. P. (1987) Structure of the high-affinity binding site for noncompetitive blockers of the acetylcholine receptor: [3H]chlorpromazine labels homologous residues in the beta and delta chains. *Biochemistry* **26,** 2410–2418.
55. Revah F., Galzi J. L., Giraudat J., Haumont P. Y., Lederer F., and Changeux J. P. (1990) The noncompetitive blocker [3H]chlorpromazine labels three amino acids of the acetylcholine receptor gamma subunit: implications for the alpha-helical organization of regions MII and for the structure of the ion channel. *Proc. Natl. Acad. Sci. USA,* **87,** 4675–4679.
56. Hucho F., Oberthur W., and Lottspeich F. (1986) The ion channel of the nicotinic acetylcholine receptor is formed by the homologous helices M II of the receptor subunits. *FEBS Lett.* **205,** 137–142.
57. Pedersen S. E. Sharp S. D., Liu W. S., and Cohen J. B. (1992) Structure of the noncompetitive antagonist-binding site of the Torpedo nicotinic acetylcholine receptor. [^{3}H] meproadifen mustard reacts selectively with alpha-subunit Glu-962. *J. Biol. Chem* **267,** 10,489–10,499.
58. Revah F., Bertrand D., Galzi J. L., Devillers-Thiery A., Mulle C., Hussy N., et al. (1991) Mutations in the channel domain alter desensitization of a neuronal nicotinic receptor. *Nature* **353,** 846–849.
59. Bertrand D., Devillers-Thiery A., Revah F., Galzi J. L., Hussy N., Mulle C., et al. (1992) Unconventional pharmacology of a neuronal nicotinic receptor mutated in the channel domain. *Proc. Natl. Acad. Sci. USA* **89,** 1261–1265.
60. Akabas M. H., Stauffer D. A., Xu M., and Karlin A. (1992) Acetylcholine receptor channel structure probed in cysteine-substitution mutants. *Science* **258,** 307–310.
61. Galzi J. L., Edelstein S. J., and Changeux J. (1996) The multiple phenotypes of allosteric receptor mutants. *Proc. Natl. Acad. Sci. USA* **93,** 1853–1858.
62. Wu G., Raines D. E., and Miller K. W. (1994) A hydrophobic inhibitor of the nicotinic acetylcholine receptor acts on the resting state. *Biochemistry* **33,** 15,375–15,381.
63. Blanton M. P., Dangott L. J., Raja S. K., Lala A. K., and Cohen J. B. (1998) Probing the structure of the nicotinic acetylcholine receptor ion channel with the uncharged photoactivable compound-3H-diazofluorene. *J. Biol. Chem.* **273,** 8659–8668.
64. Armstrong N., Sun Y., Chen G. Q., and Gouaux E. (1998) Structure of a glutamate-receptor ligand-binding core in complex with kainate. *Nature* **395,** 913–917.
65. Opella S. J., Marassi F. M., Gesell J. J., Valente A. P., Kim Y., Oblatt-Montal M., et al. (1999) Structures of the M2 channel-lining segments from nicotinic acetylcholine and NMDA receptors by NMR spectroscopy. *Nat. Struct. Biol.* **6,** 374–379.
66. Oblatt-Montal M., Buhler L. K., Iwamoto T., Tomich J. M., and Montal M. (1993) Synthetic peptides and four-helix bundle proteins as model systems for the pore-forming structure of channel proteins. I. Transmembrane segment M2 of the nicotinic cholinergic receptor channel is a key pore-lining structure. *J. Biol. Chem.* **268,** 14,601–14,607.
67. Unwin N. (1995) Acetylcholine receptor channel imaged in the open state. *Nature* **373,** 37–43.
68. Blanton M. P. and Cohen J. B. (1994) Identifying the lipid-protein interface of the Torpedo nicotinic acetylcholine receptor: secondary structure implications. *Biochemistry* **33,** 2859–2872.
69. Fahr A. and Hucho F. (1986) A stopped-flow apparatus for photoaffinity labeling studies in the milliseconds time range. Application in investigations of the nicotinic acetylcholine receptor. *J. Neurosci. Methods* **16,** 29–38.
70. Johnson D. A. and Ayres S. (1996) Quinacrine noncompetitive inhibitor binding site localized on the *Torpedo* acetylcholine receptor in the open state. *Biochemistry* **35,** 6330–6336.
71. Lurtz M. M., Hareland M. L., and Pedersen S. E. (1997) Quinacrine and ethidium bromide bind the same locus on the nicotinic acetylcholine receptor from *Torpedo* californica. *Biochemistry* **36,** 2068–2075.
72. Akabas M. H. and Karlin A. (1995) Identification of acetylcholine receptor channel-lining residues in the M1 segment of the alpha-subunit. *Biochemistry* **34,** 12,496–12,500.
73. Zhang H. and Karlin A. (1997) Identification of acetylcholine receptor channel-lining residues in the M1 segment of the beta-subunit. *Biochemistry* **36,** 15,856–15,864.
74. Kim J. and McNamee M. G. (1998) Topological disposition of Cys 222 in the alpha-subunit of nicotinic acetylcholine receptor analyzed by fluorescence-quenching and electron paramag-

netic resonance measurements. *Biochemistry,* **37,** 4680–4686.
75. Ortells M. O. and Lunt G. G. (1994) The transmembrane region of the nicotinic acetylcholine receptor: is it an all-helix bundle? *Receptors Channels* **2,** 53–59.
76. Ortells M. O., Barrantes G. E., Wood C., Lunt G. G., and Barrantes F. J. (1997) Molecular modelling of the nicotinic acetylcholine receptor transmembrane region in the open state. *Protein Eng* **10,** 511–517.
77. Kotzyba-Hibert F., Kapfer I., and Goeldner M. (1995) Recent trends in photoaffinity labeling. *Angew. Chem. Int. Ed. Engl.* **34,** 1296–1312.
78. Chatrenet B., Kotzyba-Hibert F., Mulle C., Changeux J. P., Goeldner M. P., and Hirth C. (1992) Photoactivatable agonist of the nicotinic acetylcholine receptor: potential probe to characterize the structural transitions of the acetylcholine binding site in different states of the receptor. *Mol. Pharmacol.* **41,** 1100–1106.
79. Kotzyba-Hibert F., Kessler P., Zerbib V., Bogen C., Snetkov V., Takeda K., et al. (1996) Novel photoactivatable agonist of the nicotinic acetylcholine receptor of potential use for exploring the functional activated state. *J. Neurochem.* **67,** 2557–2565.
80. Alcaraz M. L., Peng L., Klotz P., and Goeldner M. (1996) Synthesis and properties of photoactivatable phospholipid derivatives designed to probe the membrane-associated domains of proteins. *J Org Chem* **61,** 192–201.
81. Kotzyba-Hibert F., Kessler P., Zerbib V., Grutter T., Bogen C., Takeda K., et al. (1997) Nicotinic acetylcholine receptor labeled with a tritiated, photoactivatable agonist: a new tool for investigating the functional, activated state. *Bioconjug. Chem.* **8,** 472–480.
82. Grutter T., Goeldner M., and Kotzyba-Hibert F. (1999) Nicotinic acetylcholine receptor probed with a photoactivatable agonist: improved labeling specificity by addition of Ce^{IV}/glutathione. Extension to laser flash photolabeling *Biochemistry* **38,** 7476–7484.
83. Huganir R. L. and Greengard P. (1990) Regulation of neurotransmitter receptor desensitization by protein phosphorylation. *Neuron* **5,** 555–567.